

Asymmetric chiral metamaterial circular polarizer based on twisted split-ring resonator

Yong Zhi Cheng · Yan Nie · Zheng Ze Cheng ·
Xian Wang · Rong Zhou Gong

Received: 22 June 2013 / Accepted: 13 September 2013 / Published online: 28 September 2013
© Springer-Verlag Berlin Heidelberg 2013

Abstract An asymmetric chiral metamaterial (CMM) circular polarizer based on bilayer twisted split-ring resonator structure was proposed and investigated. Both numerical simulations and experiments reveal that when a y-polarized wave is incident on this CMM propagating along backward ($-z$) direction, the two linear components of the transmitted wave have nearly equal amplitudes and $90^\circ(-90^\circ)$ phase difference at the resonant frequencies. This means that the right-hand circular polarization and left-hand circular polarization are realized in transmission at 6.4 and 8.1 GHz, respectively. The surface current distributions are studied to illustrate the transformation behavior for both circular polarizations. Further, the influences of the structural parameters of the circular polarizer to the transformation transmissions spectra have been investigated numerically.

1 Introduction

Over the past decade, metamaterials (MMs) have been proposed and investigated widely for their exotic electromagnetic (EM) or optical properties, which cannot be found in nature [1]. Hence, MMs could offer myriad ingredients and options beyond conventional EM materials,

which are potentially useful for manipulating polarization of EM waves [2]. Recently, the vast attention has been paid to the research of chiral metamaterials (CMMs) due to their attractive EM (optical) properties such as giant optical activity, strong circular dichroism (CD) effect, negative refractive index and asymmetric transmission effect [3–6]. CMMs are MMs composed of unit cells without any mirror symmetry, the degeneracy of the two circularly polarized waves is broken, i.e., refractive indices of right circularly polarized (RCP, +) waves and left circularly polarized (LCP, –) waves are different [7]. Thus, RCP wave and LCP wave would encounter different transmission coefficients at the resonances.

Especially, CMMs can be used to design various polarization transformers and manipulate polarization states of EM waves for achieving polarization conversion. Generally, there are two categories of CMMs: 3D stereostructures and 2D planar structures [8–11], which could achieve conversion of different polarization states of incident EM waves by proper geometrical parameter design, such as linear to linear [12–15], linear to circular [16–18], and circular to circular [19]. It is notable that the EM coupling effect among these 3D or 2D chiral structures is instrumental for polarization conversion. Based on coupling effect between two twisted resonator structures, giant optical activity, CD effect and the conversion of polarization can be realized [20, 21]. The simplest artificial 3D chiral structures like the helix wire spring or the swiss role, which could lead to circular birefringence and circular dichroism or the conversion of different polarization states. These 3D chiral structures can contribute to huge chirality and relatively wide frequency band, however, which has big thickness and is hard to fabricate and integrate into present systems. The 2D planar chiral structures include single-layer, bilayer and multi-layer structures that could

Y. Z. Cheng · Y. Nie · X. Wang · R. Z. Gong (✉)
School of Optical and Electronic Information,
Huazhong University of Science and Technology,
Wuhan 430074, People's Republic of China
e-mail: rzhgong@mail.hust.edu.cn; cyz0715@126.com

Y. Z. Cheng · Z. Z. Cheng
School of Electronic and Information Engineering,
Hubei University of Science and Technology,
Xianning 437100, People's Republic of China

be fabricated easily in practical application. Circular polarization is an important property of EM or optical wave which has many potential applications, such as antennas [22, 23], liquid crystal displays and remote sensors [24, 25]. Several efforts have been made to design various high-performance circular polarizers [10, 16–18], which can transform incident linearly polarized waves into transmitted circularly polarized waves with different directions of rotation at resonances.

In this article, we report a simple design of the circular polarizer based on bilayer twisted SRR structure asymmetric CMM. When a y -polarized wave is incident on this asymmetric CMM slab propagating along backward ($-z$) direction, we can obtain transmitted RCP and LCP waves at 6.4 and 8.1 GHz, respectively. Experiment and simulation calculations are in good agreement, and the difference in level between the transmitted waves with RCP and LCP is more than 40 dB at resonances. The physical mechanism could be further illustrated by simulated surface current distributions. The relationship between the resonant positions and the structure parameters is also studied numerically.

2 Design, simulation and experiment

Figure 1 shows the layout of the proposed structure which consists of double-layered copper structure patterned on opposite sides of an FR-4 board. The single-layer planar structure design proposed here is similar to those in [26–28]; however, it is distinguished in that bilayer asymmetry is introduced to modify the transmission for the y -polarization normal incidence. Although this single-layer SRR structure could achieve giant CD effect, which require an oblique incidence. As shown in Fig. 1a, for the unit cell structure, the front SRR is rotated 90° with respect to the back one. This unit cell can be repeated to create a layer

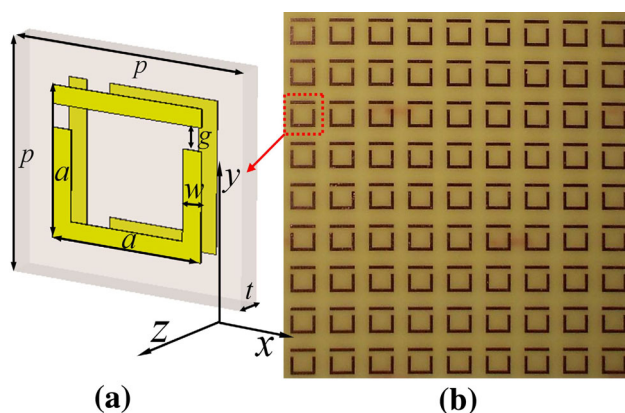


Fig. 1 Schematics of designed structure: **a** perspective view of the unit cell structure, **b** portion photography of the tested sample

that can function as a polarizer. The relative dielectric constant of the FR-4 board is 4.2 with a dielectric loss tangent of 0.02. The metallic structure layers in both sides were modeled as a 0.035-mm copper film with an electric conductivity $\sigma = 5.8 \times 10^7$ S/m. The optimal geometry parameters are as follow: $p = 10$ mm, $l = 6.4$ mm, $w = 0.8$ mm, $g = 1.2$ mm and $t = 1.43$ mm. The numerical simulations were performed based on the standard finite difference time domain method. In the process of simulation, the periodic boundary conditions were applied to the x and y directions, while perfectly matched layers were applied to the z direction.

The designed structures with a dimension of 20×20 unit cells (200 mm \times 200 mm \times 1.5 mm) was fabricated by the conventional PCB process, and the photograph of portion of a fabricated sample is shown in Fig. 1b. Then, an Agilent PNA-X N5244A vector network analyzer connected to two standard gain broadband linearly polarized horn antennas that produced microwaves in the range of 5–10 GHz was employed to measure the sample in an EM anechoic chamber. A linearly polarized EM wave (E field in the y) direction is incident on the front metallic layer, propagating along backward ($-z$) direction. On the back side, we could obtain the transmitted coefficients (t_{xy} and t_{yy}) in the x -polarization and y -polarization by rotating the received horn antennae.

3 Results and discussions

Due to the lack of the fourfold symmetry, the cross-transmission coefficients are different for incident y -polarized and x -polarized waves ($t_{xy} \neq t_{yx}$) [18]. However, the structure provides circular polarization only if the incident wave is y -polarized. In order to demonstrate the polarization conversion characteristics of the transmitted wave, the ratio $p_y = |t_{xy}|/|t_{yy}|$ and phase difference $\varphi_y = \arg(t_{xy}) - \arg(t_{yy})$ of the cross-polarization transmission t_{xy} and copolarization transmission t_{yy} are obtained for normal incident y -polarized wave by simulation and experiment, and the corresponding results are presented in Fig. 2. It is clear that the experimental results are in good agreement with simulations. It can be seen that the values of ratio p_y near unity around resonant frequencies of 6.4 and 8.1 GHz, respectively. We can conjecture that the resonances in Fig. 2a, b correspond to the frequencies where the EM coupling between the top and bottom layers is very strong. As shown in Fig. 2c, d, the phase differences between t_{yy} and t_{xy} are 90.2° and -90.6° at 6.4 and 8.1 GHz, respectively, which means that a nearly pure circular polarization wave is formed. These results prove that the transmitted waves are RCP and LCP waves at 6.4 and 8.1 GHz, respectively.

Fig. 2 Simulation and experimental linear polarization transmission coefficients for the designed CMM: **a** and **b** ratio of magnitudes p_y of t_{xy} and t_{yy} , **c** and **d** phase difference ϕ_y between t_{xy} and t_{yy}

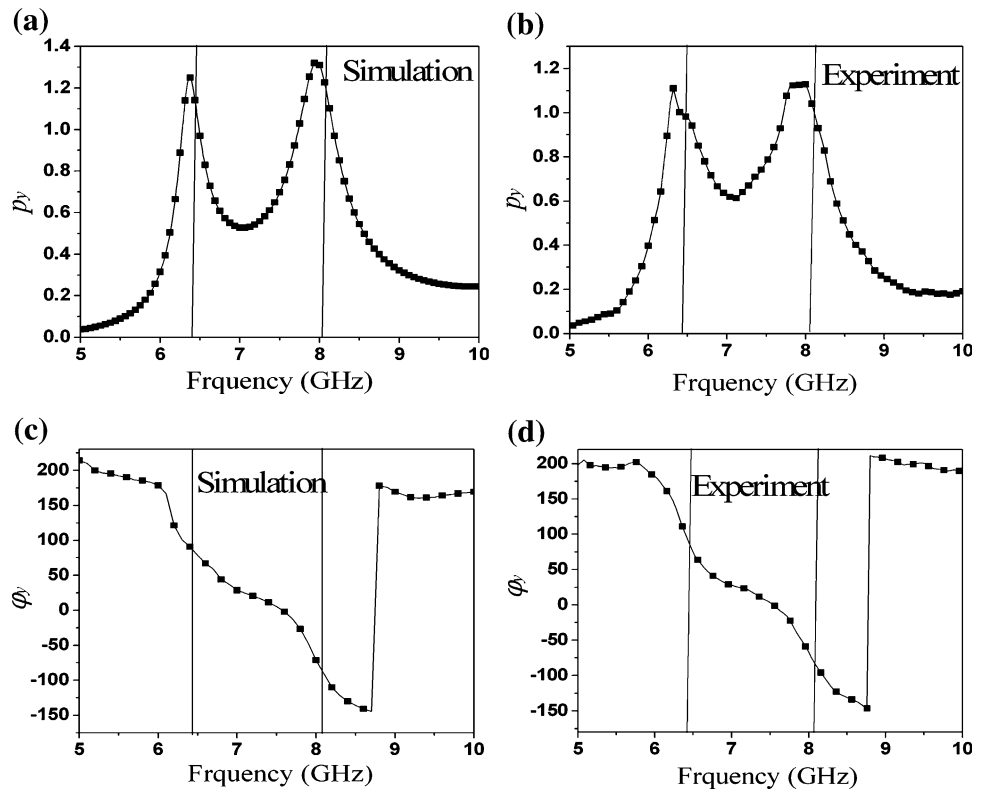


Fig. 3 **a** Simulated and **b** experimental results for the linear-circular transmission coefficients, **c** simulated and **d** experimental difference between the transmitted LCP and RCP waves

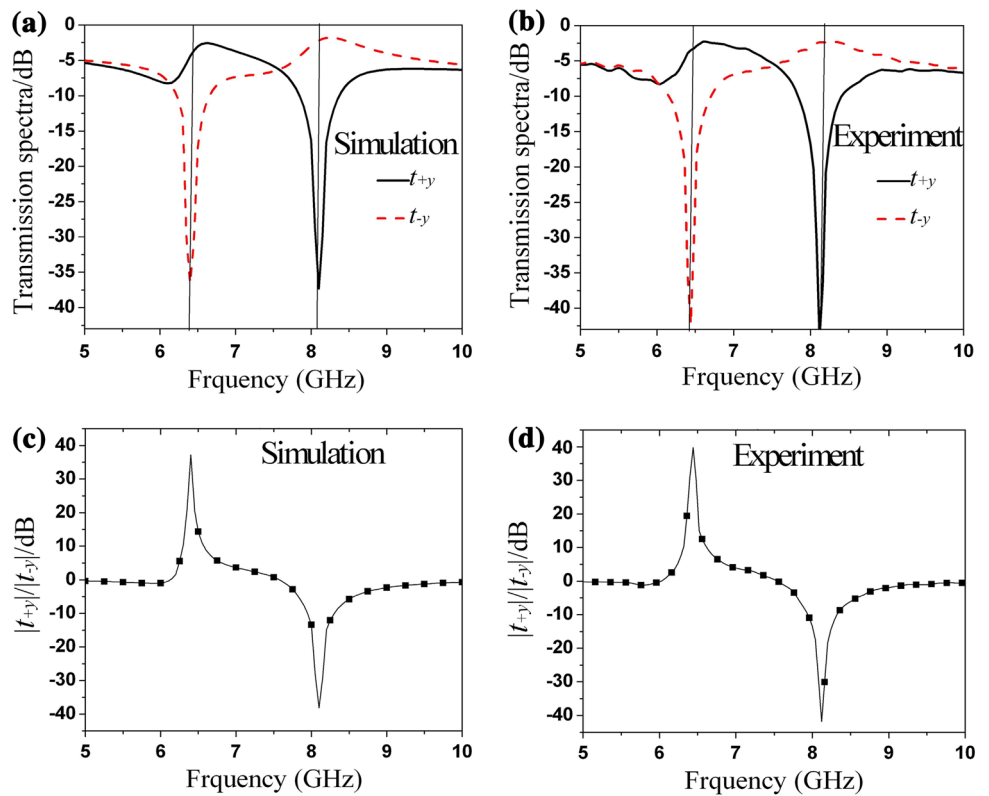
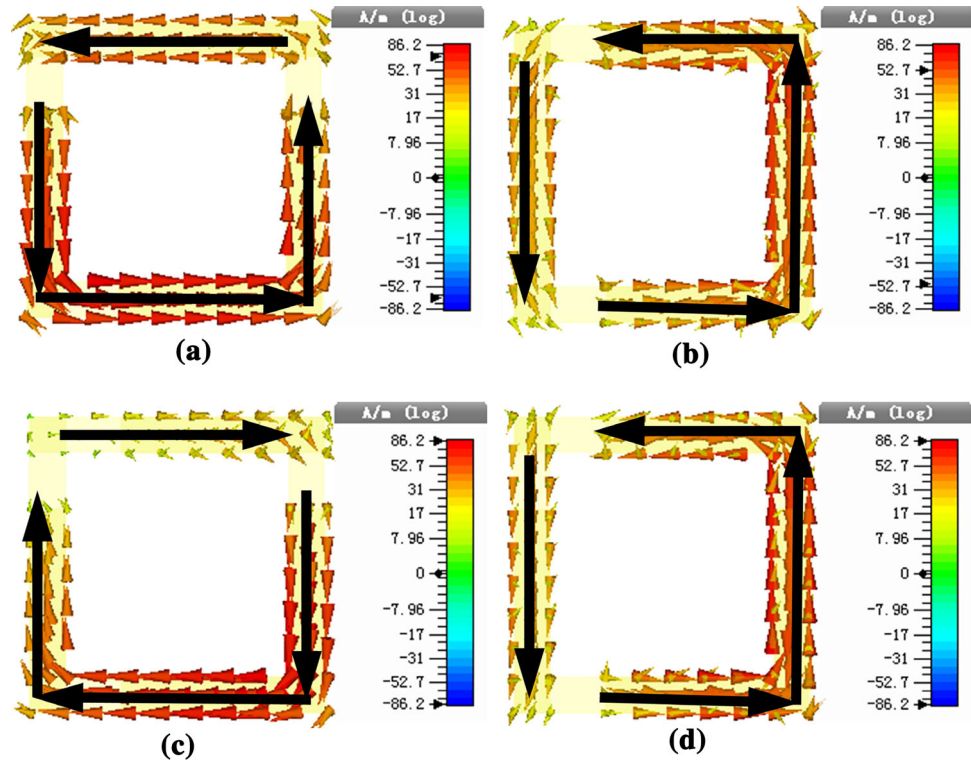


Fig. 4 Instantaneous surface current distributions induced in bilayer twisted SRRs structure for normal incident y -polarized wave **a** on top layer at 6.4 GHz and **b** on bottom layer at 6.4 GHz, **c** on top layer at 8.1 GHz and **d** on bottom layer at 8.1 GHz



The linear-circular transmission coefficients can be calculated from the t_{yy} and t_{xy} . Thus, the RCP and LCP transformation coefficients (t_{+y} and t_{-y}) can be expressed as $t_{\pm y} = \frac{1}{\sqrt{2}}(t_{xy} \pm it_{yy})$ for normal incident y -polarized wave, where the constant $\frac{1}{\sqrt{2}}$ is a result of power normalization [18]. The elements in this linear-circular transmission coefficient involve the ability of designed MMs to transform an incident linearly polarized wave into a transmitted circular wave. Figure 3a, b shows the simulation and experiment linear-circular transmission coefficients of the designed structure for incident y -polarized wave. It can be clearly seen that the designed CMM slab shows large differences in the circular polarization transmitted waves. The magnitude of the RCP wave is -2.7 and -44 dB at 6.4 and 8.1 GHz, respectively (see Fig. 3b), while the magnitude of the LCP wave is -42 and -2.3 dB at 6.4 and 8.1 GHz, respectively (see Fig. 3b). Furthermore, the ratios between the two circular polarizations transmitted wave amplitudes are shown Fig. 3c, d. One can clearly see that the difference between the transmitted waves with different circular polarization can reach a level of more than 40 dB. These results further confirm that relative pure circularly polarized waves with different rotation are realized at two frequencies, e.g., the transmitted wave is RCP at 6.4 GHz and the transmitted LCP wave is formed at 8.1 GHz. Thus, the proposed CMM slab could be used as an ultrathin ($<\lambda/24$) circular polarizer.

To better understand the physical origin of this circular polarization transformation, surface current distributions of the proposed structure are studied at the resonant frequencies for normal incident y -polarized wave. In Fig. 4a, b, at 6.4 GHz, one can see that the surface currents on the twisted SRR pairs are in the same direction, which is a symmetric resonance mode and leading to electrical dipole moments. That is, when the linearly y -polarized wave incidents along $-z$ direction, the fundamental electric resonance mode (similarly to the electric dipole mode) of the first SRR can be excited efficiently at 6.4 GHz with strong EM wave being coupled into the structure, and then the near-field coupling (electric coupling) between the first and the second SRR results in a transmitted RCP wave. As shown in Fig. 4c, d, at 8.1 GHz, the antiparallel current exists on the top and bottom layers of twisted SRRs structure, which is an asymmetric resonance mode and similar to antiparallel magnetic dipole moments. This means that the same electric dipole mode of the first SRR can be excited efficiently at 8.1 GHz with strong EM wave being coupled into the structure, but the near-field coupling (magnetic coupling) between the first and the second SRR results in a transmitted LCP wave. Thus, we can conjecture that the lower frequency transmitted RCP wave is caused by the symmetric electrical dipole resonance mode, while the higher frequency transmitted LCP is attributed to the asymmetric magnetic dipole resonance mode [29]. These current distributions characteristics effectively explain different transmitted circular polarizations.

Fig. 5 Transformation coefficients spectra for different dielectric layer thickness t **a** transformation of RCP wave, **b** transformation of LCP wave

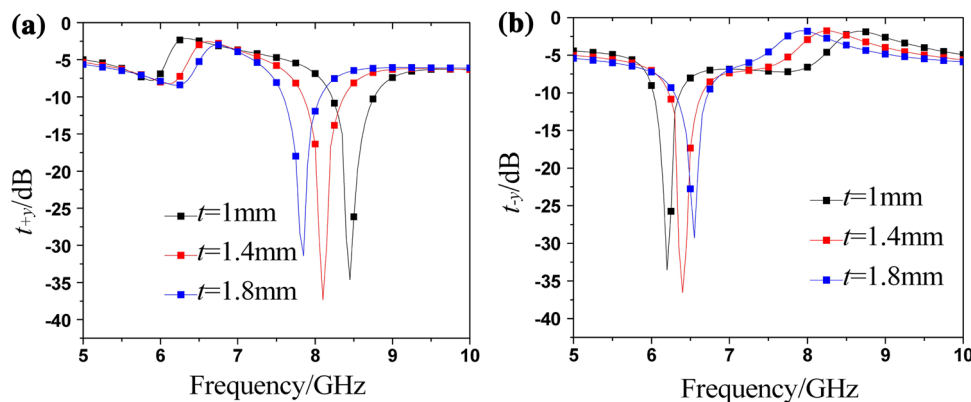
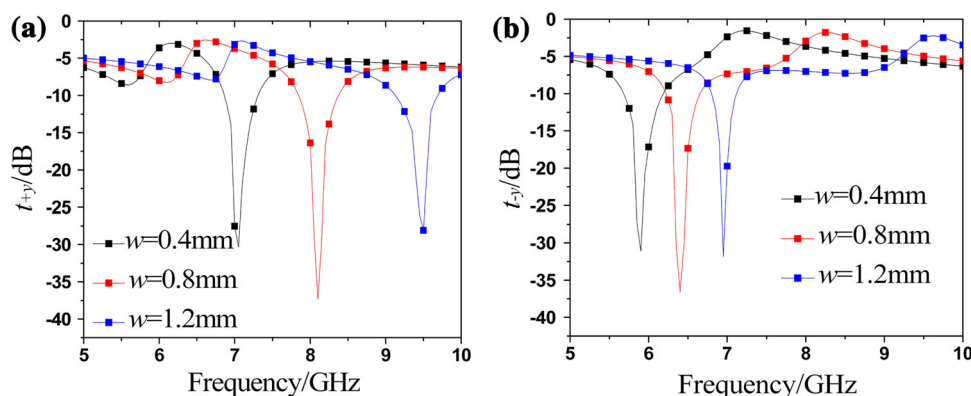


Fig. 6 Transformation coefficients spectra with different width w **a** transformation of RCP wave, **b** transformation of LCP wave



Taking a further step, the analysis of the parameters is carried out by varying one parameter while keeping the other parameters fixed. Firstly, structures with different dielectric layer thickness t (t was selected as 1, 1.4 and 1.8 mm) were calculated, while the other parameters are unchanged. Fig. 5a, b presents the transformation coefficients spectra for RCP and LCP waves with different values of t . For transformation of RCP, the positions of frequencies shift toward higher frequency when t increases. In contrast, the positions of frequencies for LCP wave shift toward lower frequency when t increases. It should be noted that the difference between the transmitted waves with different circular polarization will decrease when t increases, which mainly originate from the weak of coupling effects between two sets of the designed structure. Thus, there is limitation for the t [30]. For too large structure layer separation, coupling effects in each pair vanish and so do circular polarization transformation.

Secondly, we simulated structures with different width w ($w = 0.4, 0.8$ and 1.2 mm), while the other parameters are kept the same above. Figure 6 depicts the transformation spectra with different width w . One can clearly see that the resonant positions for LCP and RCP waves all shift toward higher frequency while w increases. The mechanism of frequency shift is easy to understand by the L-C resonance circuit theory [30].

From above simulated analyses of the designed circular polarizer, we can conclude that the circular polarization transformation can achieve tunability by changing the geometrical parameters. Thus, it is expected to design a dual-band or multi-band circular polarizer by combining different sized twisted SRR structure in a unit cell.

4 Conclusion

In conclusion, we have designed an ultrathin (the total thickness is smaller than $\lambda/24$) circular polarization transformer based on bilayer twisted SRR structure. Both simulation and experiment exhibit that this simple structure can convert a linearly y -polarized wave to an RCP wave and LCP wave at 6.4 and 8.1 GHz, respectively. The difference between transmitted circular polarization wave levels can reach more than 40 dB, which is larger than the previous reported design [16–18]. The physical mechanism behind the phenomena is illustrated by simulating surface current distributions of the unit cell structure. The generation mechanism of RCP wave of the lower frequency is mainly due to the local electric dipoles resonance, and the LCP wave of the higher frequency is mainly from the local magnetic dipoles resonance. Furthermore, the influences of the structural parameters of the circular polarizer also have

been investigated numerically. A dual-band or multi-band circular polarizer design could be expected by combining different sized twisted SRR structure in a unit cell. In addition, the proposed structure could be operated at other higher frequency bands by scaling down the geometric dimensions, such as terahertz or even optical range.

Acknowledgments This work is supported by the National Natural Science Foundation of China (51207060).

References

1. D.R. Smith, J.B. Pendry, M.C.K. Wiltshire, *Science* **305**, 788 (2004)
2. A.V. Rogacheva, V.A. Fedotov, A.S. Schwanecke, N.I. Zheludev, *Phys. Rev. Lett.* **97**, 177401 (2006)
3. E. Plum, J. Zhou, J. Dong, V.A. Fedotov, T. Koschny, C.M. Soukoulis, N.I. Zheludev, *Phys. Rev. B* **79**, 035407 (2009)
4. S. Zhang, Y.S. Park, J. Li, X. Lu, W. Zhang, X. Zhang, *Phys. Rev. Lett.* **102**, 023901 (2009)
5. J. Zhou, J. Dong, B. Wang, Th. Koschny, M. Kafesaki, C.M. Soukoulis, *Phys. Rev. B* **79**, 121104(R) (2009)
6. X. Xiong, W.H. Sun, Y.J. Bao, M. Wang, R.W. Peng, C. Sun, X. Lu, J. Shao, Z.F. Li, N.B. Ming, *Phys. Rev. B* **81**, 075119 (2010)
7. J.D. Jackson, *Classical Electrodynamics*, 3rd edn. (Wiley, New York, 1999)
8. C.M. Soukoulis, M. Wegener, *Nat. Photonics* **5**, 523 (2011)
9. B. Bai, Y. Svirko, J. Turunen, T. Vallius, *Phys. Rev. A* **76**(2), 023811 (2007)
10. J.K. Gansel, M. Thiel, M.S. Rill, M. Decker, K. Bade, V. Saile, G. Freymann, S. Linden, M. Wegener, *Science* **325**, 1513 (2009)
11. C. Wu, H. Li, X. Yu, F. Li, H. Chen, C.T. Chen, *Phys. Rev. Lett.* **107**, 177401 (2011)
12. Y. Ye, S. He, *Appl. Phys. Lett.* **96**, 203501 (2010)
13. J. Han, H.Q. Li, Y.C. Fan, Z.Y. Wei, C. Wu, Y. Cao, X. Yu, F. Li, Z.S. Wang, *Appl. Phys. Lett.* **98**, 151908 (2011)
14. C. Huang, Y. Feng, J. Zhao, Z. Wang, T. Jiang, *Phys. Rev. B* **85**, 195131 (2012)
15. Y.Z. Cheng, Y. Nie, X. Wang, R.Z. Gong, *Appl. Phys. A Mater. Sci. Process.* **111**, 209 (2013)
16. M. Mutlu, A.E. Akosman, A.E. Serebryannikov, E. Ozbay, *Opt. Lett.* **36**, 1653 (2011)
17. X. Ma, C. Huang, M. Pu, C. Hu, Q. Feng, X. Luo, *Opt. Express* **20**, 16050 (2012)
18. S. Yan, G.A.E. Vandenbosch, *Appl. Phys. Lett.* **102**, 103503 (2013)
19. L. Wu, Z.Y. Yang, Y.Z. Cheng, Z.Q. Lu, P. Zhang, M. Zhao, R.Z. Gong, X.H. Yuan, Y. Zheng, J.A. Duan, *Opt. Express* **21**, 5239 (2013)
20. Nasimuddin, X. Qing, Z.N. Chen, *IEEE Trans. Antenna Propagat.* **59**, 285 (2011)
21. H. Liu, D.A. Genov, D.M. Wu, Y.M. Liu, Z.W. Liu, C. Sun, S.N. Zhu, X. Zhang, *Phys. Rev. B* **76**, 073101 (2007)
22. H. Liu, Y.M. Liu, T. Li, S.M. Wang, S.N. Zhu, X. Zhang, *Phys. Status Solidi B* **246**, 1397 (2009)
23. D. Zarifi, H. Oraizi, M. Soleimani, *Prog. Electromagn. Res.* **123**, 337 (2012)
24. Q. Hong, T. Wu, X. Zhu, R. Lu, S.T. Wu, *Opt. Express* **13**, 8318 (2005)
25. Z. Ge, M. Jiao, R. Lu, T.X. Wu, S.T. Wu, W.Y. Li, C.K. Wei, *J. Display Technol.* **4**, 129 (2008)
26. E. Plum, X.X. Liu, V.A. Fedotov, Y. Chen, D.P. Tsai, N.I. Zheludev, *Phys. Rev. Lett.* **102**, 113902 (2009)
27. N.I. Zheludev, E. Plum, V.A. Fedotov, *Appl. Phys. Lett.* **99**, 171915 (2011)
28. C. Feng, Z.B. Wang, S. Lee, J. Jiao, L. Li, *Optics Commun.* **285**, 2750 (2012)
29. Z.Y. Cheng, Y. Nie, L. Wu, R.Z. Gong, *Prog. Electromagn. Res.* **138**, 432 (2013)
30. Y.B. Ding, G.P. Zhang, Z.Y. Cheng, *Phys. Scr.* **85**, 065405 (2012)